Supplementary material for

Transferable Coarse-Grained Models of Liquid-Liquid Equilibrium Using Local Density Potentials Optimized with the Relative Entropy

Tanmoy Sanyal and M. Scott Shell

University of California Santa Barbara, Santa Barbara, California

A. Transferability of pair correlations and local density distributions using different CG models

Fig. S1-S5 present the comparison between all-atom (AA, black dots) and CG radial distribution functions (RDFs, of types BB and WW) and local density (LD) distributions (of types BB, WW and WB) for the different CG forcefields in Table 1 in the paper. CG models for various combination of these LD potentials are parameterized from reference compositions of 10%, 50% and 90% benzene mole fraction (dark framed plot, along the rows). CG models constructed at a particular atomistic reference are used in MD simulations of mixtures from 10% to 90% composition (along the columns), which are then used to calculate and compare RDFs and LD distributions with corresponding AA MD simulations at these compositions.

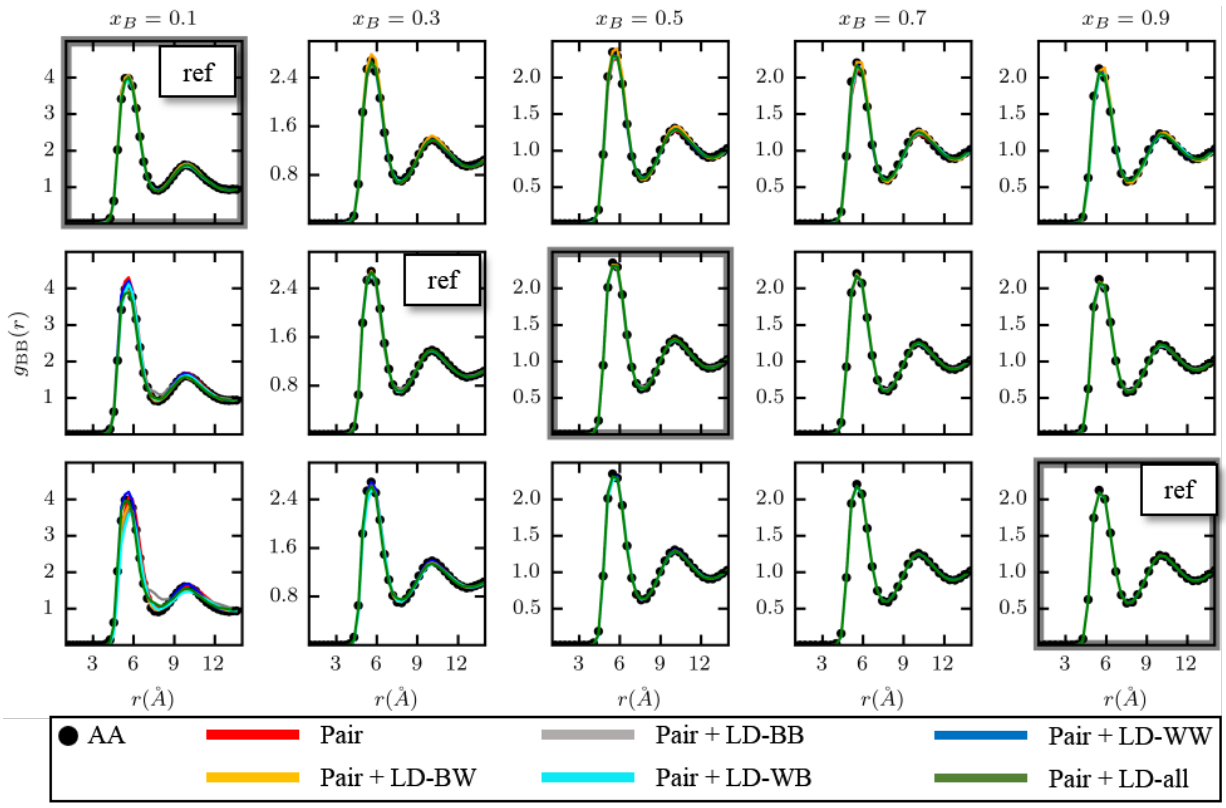

FIG S1. B-B RDFs

All CG forcefields, even the ones with only pair interactions, demonstrate excellent transferability for the BB pair correlations. This is consistent with the fact that the BB pair potential changes only slightly when re-parameterized in the presence of the LD-BB potential (Fig. 4 in paper).

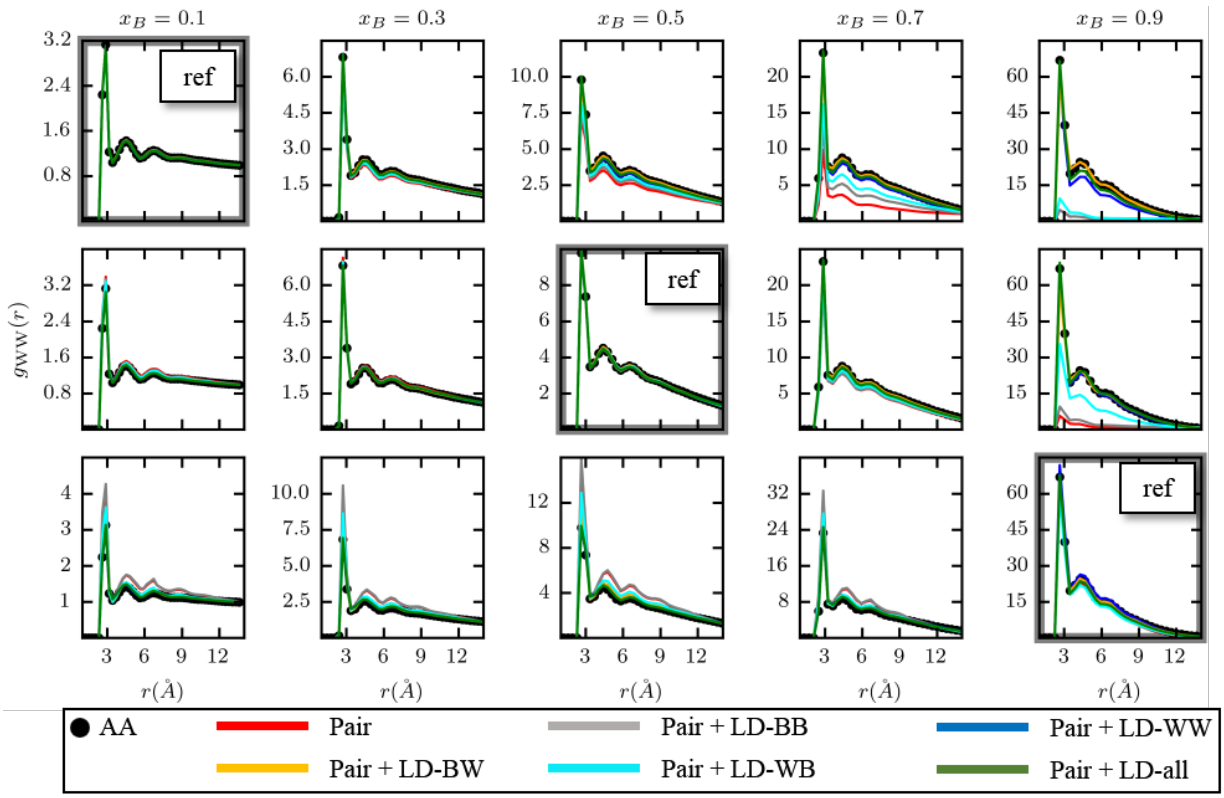

FIG S2. W-W RDFs

The W-W pair correlations have more pronounced changes in transferability when going from a CG model with only pair potentials to those with LD potentials. The small effect of the B-B many-body interactions is demonstrated by the poor transferability of the Pair + LD-BB model, similar to that of the Pair-only CG model. Both of these models have good representability at the reference composition but under-predict the significant water-water association at higher compositions. The unusually high magnitudes of the RDF peak at all compositions $\geq 30\%$ reflect the formation of tight water clusters, modulated by the overall bulk density of the system. The LD-WB potential also under-predicts the distribution peaks in dense solutions. The Pair + LD-WW and Pair + LD-all CG models have the best transferability, quantitatively reproducing the RDFs at all compositions.

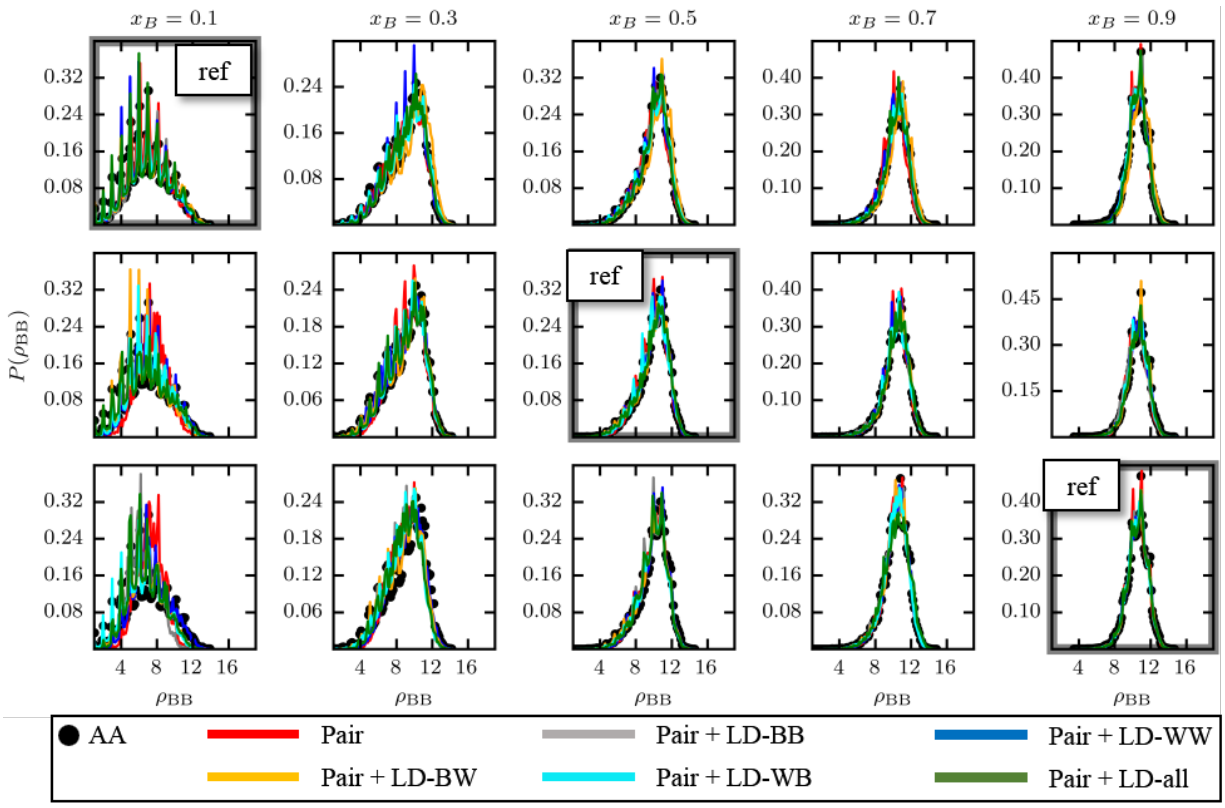

FIG S3 B-B LD distributions

Transferability for the B-B LD distributions follow similar trends to those for the corresponding pair correlations. However, there are some differences in representability. The pair-only CG model fails to represent the distribution even for the composition at which it was parameterized. All CG models that include one or more LD potentials have similar transferability, for each reference composition. The jagged peaks throughout the upper contour of the distribution at 10% are due to the discrete nature of the indicator function φ (Eq. 3 in paper) used to determine the local density, as discussed in detail in Ref. 1. Higher benzene compositions add more counts to the LD BB histogram, thus further smoothening out these jagged peaks.

The typical number of benzene neighbors around a CG benzene site grows from ~ 6 in the 10% solution to ~ 11 in the 90% solutions. From this and from the B-B RDFs in Fig. S1, we

hypothesize that B-B pair structure in the more concentrated solutions (≥ 30%) closely mimics that of a simple liquid. This might explain why this BB LD distribution or the BB RDF (Fig. S1) are reproduced reasonably across most of the composition space by the Pair-only model alone without the need for multibody interactions to accurately represent the missing orientational degrees of freedom.

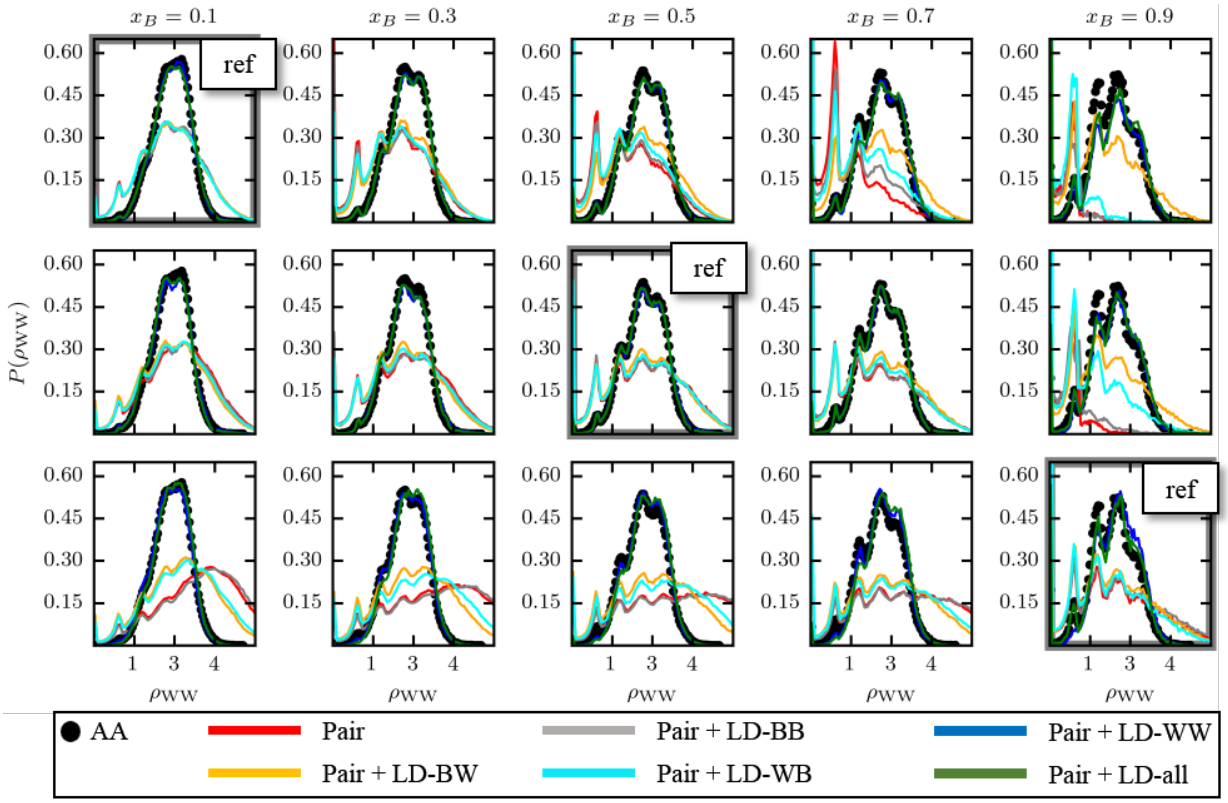

FIG S4. W-W LD distributions

The W-W LD distribution is particularly sensitive to the presence of the LD-WW potential. For each parameterization reference, only two CG models, Pair + LD-WW and Pair + LD-all can reproduce the distribution across the entire range of compositions. All other CG models severely under-predict both the location of the peak and its spread. As discussed in the paper, the LD-WW potential is arguably the most important LD potential to retain in CG models presented in this

work. Also notice that the peak values are ~ 1.5-2 times larger than the B-B LD distributions in Fig. S3, thus pointing to very tight water clusters, compared to benzene association.

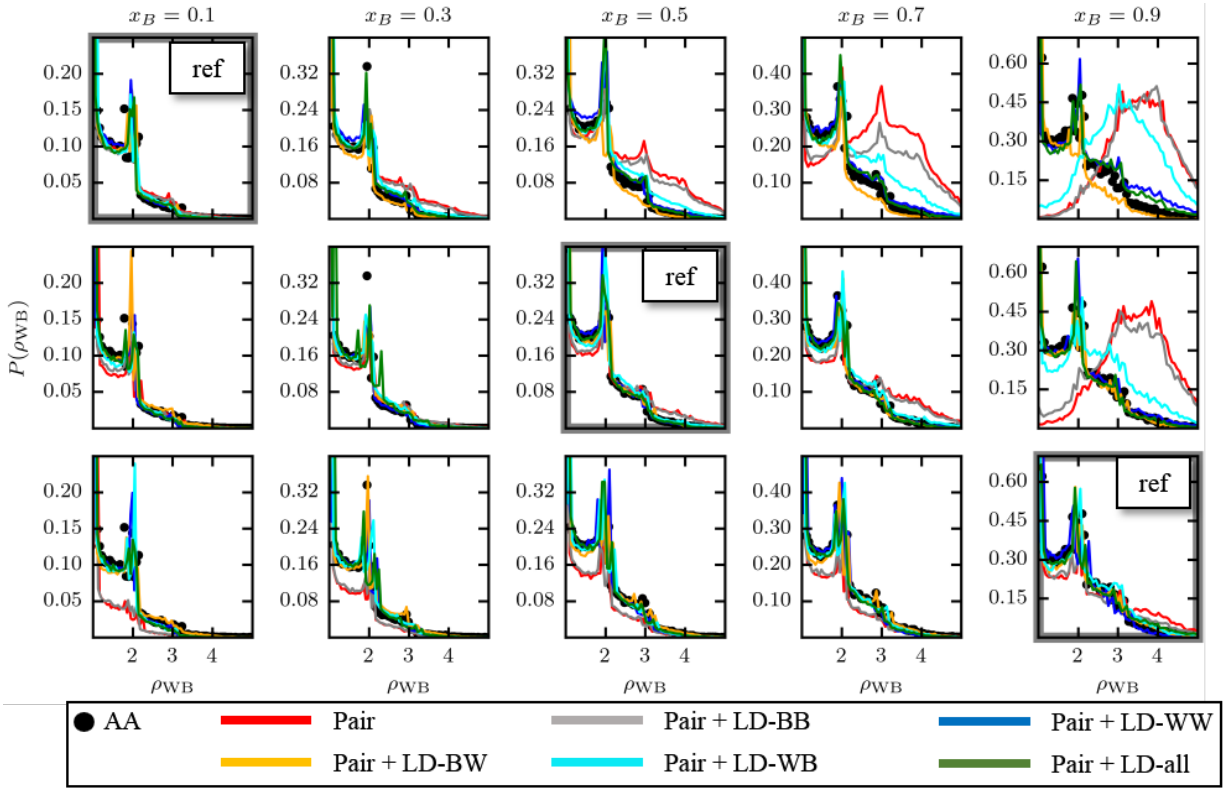

FIG S5. W-B LD distributions

Transferability of the W-B LD distribution is best for the Pair + LD-all forcefield and reasonably good for the Pair + LD-WW. The Pair-only and Pair + LD-BB forcefields produce distributions that scale very poorly across composition space. The distributions are also reproduced moderately well by the forcefield that includes only the LD-BW potential, which may be intuitive. It is therefore interesting to see that the same does not hold for the Pair + LD-WB model, which transfers poorly, significantly under-predicting both the peak and the spread at high concentrations.

B. RMS errors between AA and CG predictions of pair correlations and local density distributions using a relative deviation metric

Fig. 5 in the paper employs an average RMS error between AA and CG pair correlations and LD distributions characterized by absolute deviations i.e. $\frac{1}{N}\sum\left(X_{\alpha\beta}^{AA} - X_{\alpha\beta}^{CG}\right)^2$, where $X_{\alpha\beta} = g_{\alpha\beta}(r)$ or $P_{LD}\left(\rho_{\alpha\beta}\right)$ and N is the number of discrete histogram bins. Using absolute deviations makes this error metric sensitive to the range of the normalized histogram bin values, especially for the LD distributions. When RMS errors for different LD types (BB, WW, BW and WB) are added, models from 10% and 50% references produce a lower average error at compositions away from the reference, that can be erroneously interpreted as meaning increasingly higher transferability at state points further away from the reference. Further the average RMS errors for P_{LD} are non-zero at the reference compositions, where the AA and CG LD distributions are expected to overlap quantiatively[2], especially for the Pair + LD-WW and Pair + LD-all forcefields (Fig. 4 in paper, Figs. S1-S5)

To remove the sensitivity of the absolute RMS error to the histogram peak values, we construct an alternate RMS metric that uses relative mean square deviations normalized by the AA histogram value, namely

$$\begin{aligned} \text{RMS}\,[g(r)] &= \left(x_B^2\,\langle \Delta g_{BB}^2\rangle + \; x_W^2\,\langle \Delta g_{WW}^2\rangle + \; 2x_B x_W\,\langle \Delta g_{BW}^2\rangle\right)^{\frac{1}{2}} \\ \text{RMS}\,[P_{LD}(\rho)] &= \Big[\, x_B^2\,\langle \Delta P_{LD,BB}^2\rangle + \; x_W^2\,\langle \Delta P_{LD,WW}^2\rangle \\ &\qquad + \; x_B x_W\,\left(\langle \Delta P_{LD,BW}^2\rangle + \langle \Delta P_{LD,BW}^2\rangle\right)\Big]^{\frac{1}{2}} \end{aligned} \tag{1}$$

where

$$\langle \Delta X_{\alpha\beta}^2\rangle = \frac{1}{N}\sum\left(\frac{X_{\alpha\beta}^{AA} - X_{\alpha\beta}^{CG}}{X_{\alpha\beta}^{AA}}\right)^2 \tag{2}$$

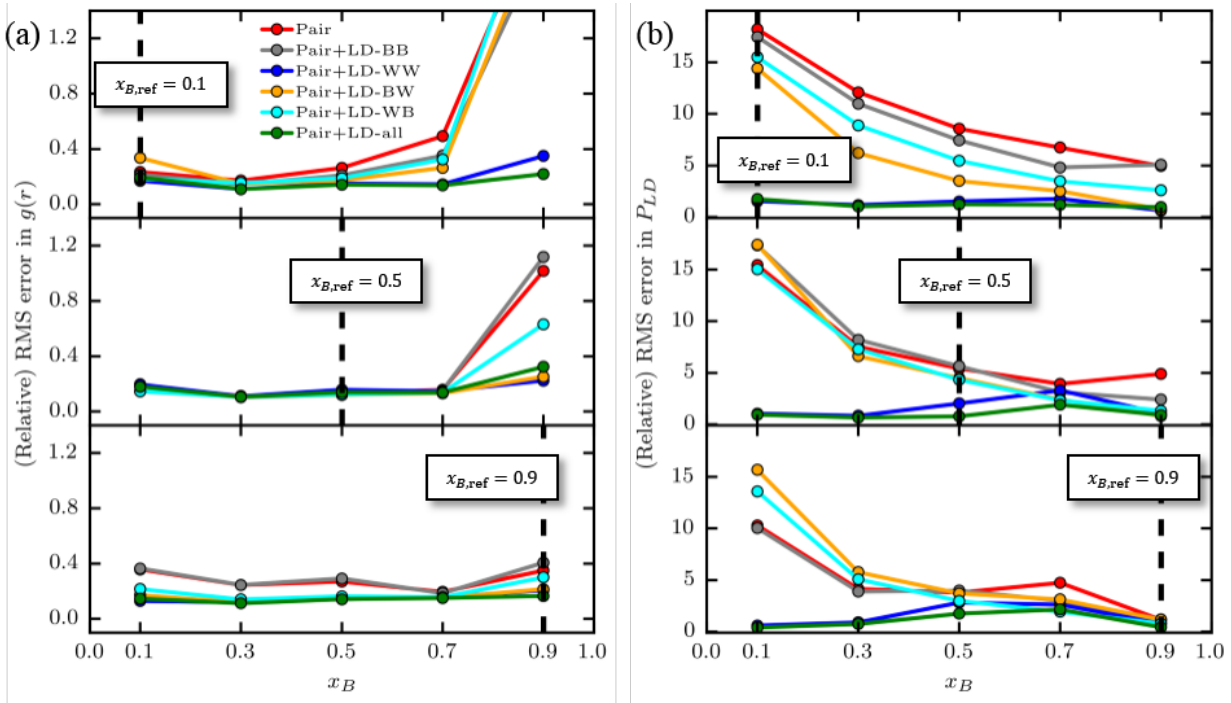

Fig. S6 Composition-weighted relative RMS overlap for (a) pair correlations and (b) local density distributions, between AA systems and CG models parameterized from 10%, 50% and 90% reference compositeions (along the vertical subpanels). Choosing a relative RMS metric reduces the sensitivity of the errors to the peak values for different types of RDFs and LD distributions and brings out the superior performance of the Pair + LD-WW and Pair + LD-all forcefields.

and, $X_{\alpha\beta} = g_{\alpha\beta}(r)$ or $P_{LD}(\rho_{\alpha\beta})$.

Fig S6 recapitulates the composition weighted RMS errors, but this time using the relative mean squared deviation in Eq. 2 above. The Y-axis ranges for the RDFs in panel (a) remain the same as in the paper, but the ranges of panel (b) increase significantly. Using relative deviations essentially magnifies the errors so that it is apparent at once that forcefields other than Pair + LD-WW and Pair + LD-all produce very large relative errors. For the LD distributions, these errors decrease by ~ 50% across the range of compositions, regardless of the reference composition. But the Pair + LD-WW and Pair + LD-all models produce average errors that are 300% lower for the RDFs and 1400% for the LD distributions and change by ~ 50% (similar to Fig 5 in the paper) across the entire range of compositions.

C. CG model transferability across different bulk densities

To test the transferability of the CG models across bulk density, we perform both AA and CG simulations of a 50% benzene mole fraction mixture using (cubic) boxes that are 10% smaller and larger than the original equilibrium dimension ($L_0 = 35.2\ 5$ Å). Although these simulations are in the NVT ensemble, they provide an idea of the model transferability across different bulk densities and thus also at different average pressures.

Fig. S7 presents a comparison of the BB, WW and BW radial distribution functions (RDFs) between the AA and CG models at these box sizes, for the 6 different forcefields outlined in Table 1 of the manuscript parameterized from the 50% mixture reference. The relative RMS errors (RMSE) between the AA and CG RDFs are calculated according to: $RMSE(X) = \left\langle \left(1 - \frac{X_{CG}}{X_{AA}}\right)^2 \right\rangle$, where $X = g_{BB}$, g_{WW} or g_{BW}. All the CG forcefields perform better at lower bulk densities as evidenced by the lower RMSE for the larger box. Interestingly, the Pair + LD-all model retains nearly the same low RMSE (~20-30 %) for the BB and BW RDFs across the higher and lower densities but has a very high RMSE for the BW RDF at higher densities.

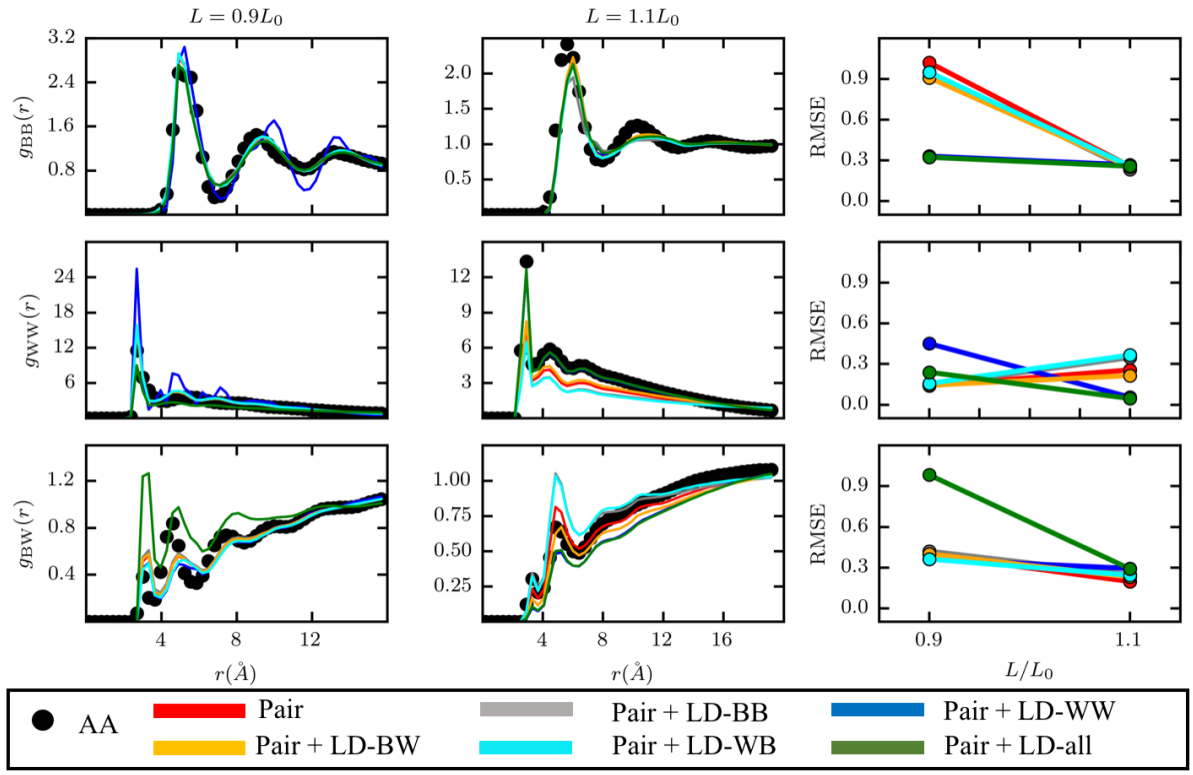

FIG. S7 BB, WW and BW radial distribution functions for the 50% benzene mole fraction at box dimensions 10% smaller (column 1) and larger (column 2) from the one tuned to produce correct equilibrium bulk density of benzene and water, i.e. at different effective pressures. Column 1 and 2 visually compare the different RDFs (each row is a different RDF type) between the AA system and the different CG models of Table 1 in the manuscript, while column 3 quantifies this comparison through a relative RMS error metric. Most CG models seem to be more transferable for the larger box size, i.e., at lower bulk density.

D. Hard sphere excess chemical potentials for the different CG models

Fig. S8 compares the excess chemical potential due for inserting a hard sphere ($\mu^{ex}(R)$) for the AA system and different CG models, at 10%, 50% and 90% references. Fig. 6 in the paper presented fractional errors between AA and CG predictions of $\mu^{ex}(R)$, while Figure S8 presents the absolute AA and CG excess chemical potentials side by side. For $R \geq 1.5$ Å, the excess chemical potential decreases (the most apparent change is ~ 2 kcal/mol for the 5 Å sphere) from low to high benzene composition, which is expected from how the hard sphere contact density is

modulated by increasing the benzene fraction in the liquid mixtures, and is elaborated in the paper (Eq. 10). The errors between AA and CG models are difficult to see in this representation and are better represented as fractional deviations presented in Fig. 6.

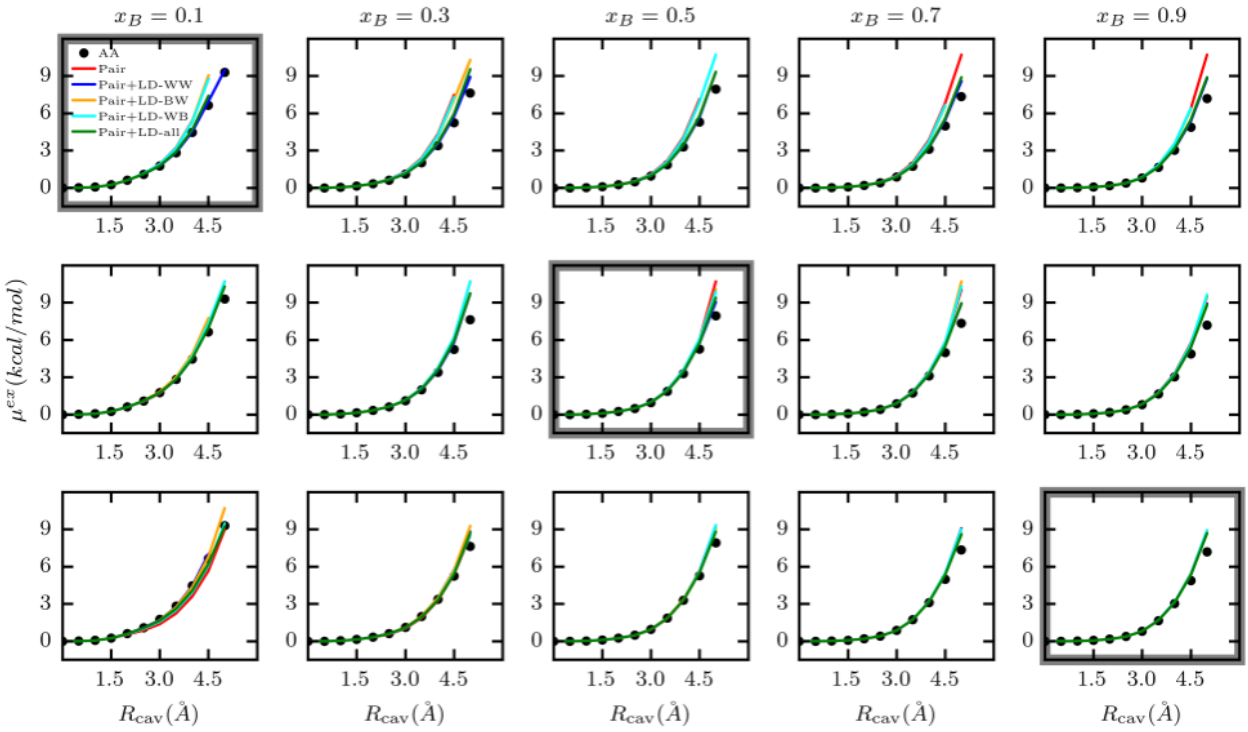

Fig. S8 Excess chemical potentials for inserting a hard sphere with diameters ranging from 0 – 5 Å, for the different CG models forcefields in Table 1 in the paper, parameterized from reference compositions of 10%, 50% and 90% benzene mole fractions (dark framed plot marked "ref" along the rows). AA values are marked with black dots.

References

(1) Sanyal, T.; Shell, M. S. Coarse-Grained Models Using Local-Density Potentials Optimized with the Relative Entropy: Application to Implicit Solvation. *J. Chem. Phys.* **2016**, *145* (3), 34109.

(2) Chaimovich, A.; Shell, M. S. Coarse-Graining Errors and Numerical Optimization Using a Relative Entropy Framework. *J. Chem. Phys.* **2011**, *134* (9), 94112.